Velocity Distributions of Camphor Particle Ensembles

Oliver Schulz and Mario Markus*

Max-Planck-Institut für molekulare Physiologie, Postfach 500247, 44202 Dortmund, Germany

Received: April 5, 2007; In Final Form: May 21, 2007

The spatial distribution of ensembles of camphor particles on a water surface can be classified into four phases with the following properties, for increasing density: (I) no clustering of particles and a minimum distance distribution similar to that of a 2D ideal gas; (II) reminiscent of a gas with clustering of particles; (III) net-like structure with occasional rearrangements; and (IV) motionless. While single particles have varying velocity distributions, the overall velocity distribution is Laplacian (the width decreasing with increasing camphor density) for all phases.

1. Introduction

There has been growing interest in creating isothermal chemomechanical transducers that mimic biological motion. In the nano- and microscales, a number of self-propelled motors have been designed mainly by attaching catalysts to differently shaped particles.[1−5] Examples at scales visible to the naked eye are the following: floating diodes in an external alternating electric field,[6] amoeba-like motions of reactive oil/water systems,[7] reactive droplets on a glass plate,[8] pentanol drops in water,[9] droplets of the Belousov−Zhabotinsky reactant in oleic acid,[10] platinum plates made to float on hydrogen peroxide,[11] grains of phenanthroline on a $FeSO_4$ solution,[12] and particles of camphor and its derivates on water. The latter has received the most intensive attention, especially by the groups working with Nakata,[13−25] who investigated the dynamics of one, two, or three particles in varying geometries and physicochemical conditions.

In this work we shall investigate the behavior of ensembles of a large number of camphor particles on a water surface. For a better understanding of this system, one should keep in mind that three kinds of forces act on the particles: (i) a force causing propulsion of each particle due to the asymmetric lowering of the surface tension (owing to dissolved camphor) around the particle; (ii) a repulsion between particles (a force acts from lower to larger surface tension and thus the dissolved camphor around a grain decelerates an approaching particle)—this repulsion is an important feature in the behavior of two camphor boats in circular, polygonal, or 8-shaped chambers;[23−25] and (iii) an attraction between particles for very small distances (smaller than the capillary length), since the surface of the two menisci decreases as the particles approach each other.[26] This latter force causes clustering of particles in our experiments; in the literature this force is found in connection with the so-called "capillary bond", which is a central concept for the mesoscopic self-assembly in molecule-mimetic chemistry.[27−29]

2. Experimental Section

Camphor (racemic) was obtained from Sigma Chemical. Due to humidity, the purchased camphor is found as large clumps in the flasks. These clumps were ground right before each experiment with a commercial electrical pepper mill (exit diameter 2.3 cm). The ground particles fell from the mill forming a cone-shaped stream that had a diameter of 5 cm when it reached the water surface. Double-distilled water was placed below the mill in a cylinder (diameter 6.3 cm; depth 4.4 cm; temperature 23 ± 1 °C). The surface tension at the air−water interface was measured by using the standard Wilhelmy method.[30]

For speed and precision, we constructed a motorized device that allowed the mill to swing away from under the video camera within 2 s. If not stated otherwise, the measuring time, T, was 600 s. None of the features given in this work change significantly during this time. In particular, the loss of camphor due to dissolution in water within T is negligible in our analyses. We used a CMOS-camera (Basler A602f-2) with a digital IEEE-1394 interface and recorded 640 × 480 pixels at $\tau = 50$ frames per sec. Misleading reflections caused by deformations of the water surface near the particles were avoided by surrounding the water surface with 40 LEDs. Optical discernment of camphor from water was done by the triangulation method.[31] A pixel indicating camphor was defined as belonging to a given particle if it was within the 8-pixel neighborhood of any of any other pixel of that particle. For each pixel, Multi-Resolution Motion Estimation (MRME) was performed.[32] By using this method, a vector $\vec{\delta}$ for the displacement of the content of each pixel is determined. The displacement vectors of all pixels corresponding to a given particle were used to determine the dynamics of that particle.

3. Results

3.1. Distributions on the Water Surface. For characterization we define the following: (a) the camphor density $\rho = M/F$, where M is the mass of the camphor supplied by the mill and F is the surface area of the water, and (b) the coverage $\beta = A/F$, where A is the total camphor-covered surface area, as registered by the camera. We define $t = 0$ as the time at which the camphor arrives on the water surface (after falling from the mill) and $t_1 = 2$ s as the time after which the mill is swung away and the experiment starts.

The distribution of sizes of the particles at $t = 0$ (before any clustering takes place on the water surface) was measured by replacing the water cylinder by a black gel at equal height as the water surface. The particles, immobilized on the gel, have the distribution shown by stars in Figure 1a. The mean diameter

* Address correspondence to this author: www.mariomarkus.com.

10.1021/jp072677f CCC: $37.00
Published on Web 06/26/2007

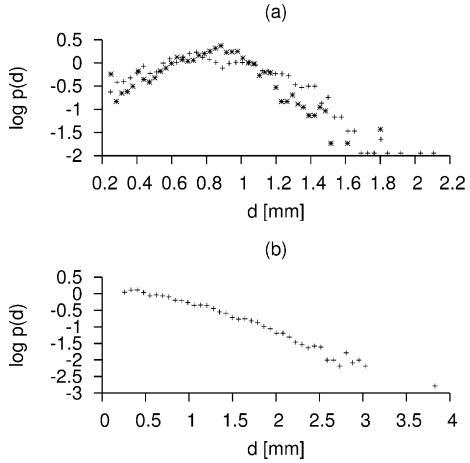

Figure 1. (a) Probability distributions of the mean particle diameter *d*. (a) $\rho = 6$ g/m^2 (phase I, Figure 2a): stars, particles right after emergence from the mill ($t = 0$); crosses, particles on the water at the start of experiments ($t = t_1$). (b) $\rho = 21$ g/m^2 (phase II, Figure 2b): distribution at the start of experiments ($t = t_1$) due to previous clustering on the water.

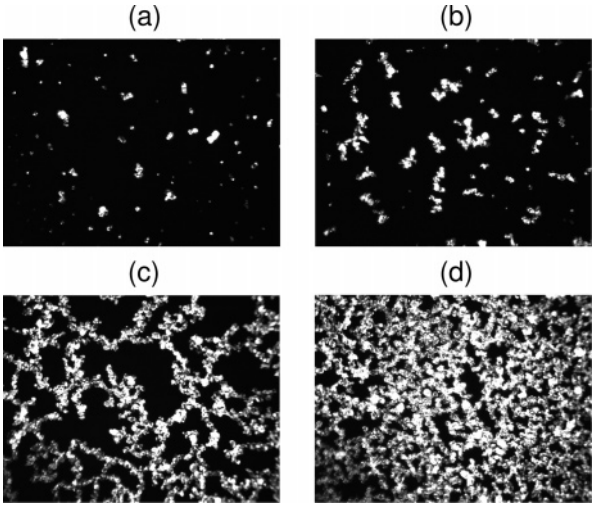

Figure 2. Spatial distributions of camphor particles. Window size: 4.4 cm × 3.3 cm. (a) $\rho = 6$ g/m^2 (phase I). (b) $\rho = 21$ g/m^2 (phase II), (c) $\rho = 55$ g/m^2 (phase III). (d) $\rho = 178$ g/m^2 (phase IV).

d of a particle (abscissas in Figure 1) is defined as $d = 2\sqrt{a/\pi}$, where *a* is the mean area of the particle.

Figure 2 shows four typical camphor distributions on the water surface. Figure 2a (lowest ρ) is a gas-like configuration, which we call "phase I". For this phase, the particle size distribution at $t = 0$ does not differ significantly from that at $t = t_1$ (see Figure 1a) and did not change afterward within the measuring time *T*. This is because no significant clustering of particles occurs in phase I. The dynamics in this phase is clearly dominated by the repulsive forces.

At larger ρ (Figure 2b), clustering takes place directly after the particles fall (partly closer than the capillary distance) from the mill on the water. This clustering occurs within the short time $t_1 = 2$ s in which the mill is swung away and clears the camera's field of view. The resulting particle size distribution is illustrated in Figure 1b. Within the following measuring time *T*, this distribution is stable owing to the repulsion between the clusters, i.e., no further significant clustering takes place. We call this configuration "phase II".

At even larger ρ (Figure 2c), we obtain what we call "phase III". In this case the configuration consists mainly of one single cluster, which has a net-like structure. During the time *T* rearrangements occur within this structure, so that the mean velocities are clearly distinguishable from zero (see Figure 4c).

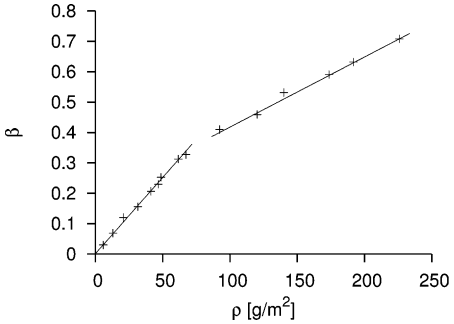

Figure 3. Coverage β versus camphor density ρ. The left straight line corresponds to phases I, II, and III. The right straight line corresponds to phase IV.

At the largest ρ in our experiments (Figure 2d) we obtain what we call "phase IV". This phase has mean velocities not significantly different from zero (as compared to phase III; see Figure 4). In contrast to the other phases, in which particles move freely and the repulsive forces play a significant role, phase IV consists of particles immobilized by the attractive forces. Phase IV can also be characterized by plotting β versus ρ (Figure 3). The straight line on the left corresponds to phases I, II, and III, while the straight line on the right corresponds to phase IV. Thus, in this latter case β grows slower as ρ is increased, as compared to the other phases, which is mainly due to compression within the spread of camphor on the water.

3.2. Velocity Distributions. Invariably, the analyses of single pixel displacements $\vec{\delta}$ yield Laplacian distributions, which are given by

$$f(v_i) = \frac{1}{2b} e^{-|v_i|/b} \tag{1}$$

where $v_i = \delta_i/\Delta t$, $i = x, y$, and $\Delta t = 0.02$ s.[33] Doubling Δt does not significantly change the results. The distributions are illustrated for phases I through IV in Figure 4. Note that the distributions become narrower around zero, as ρ increases, until nearly a δ-function is obtained for phase IV (Figure 4d). Note also that the number of points in the figures decreases for increasing ρ because v_x and v_y decrease while the resolution of the evaluation remains.

The decreasing velocity on increasing ρ, as indicated by the narrowing of the distributions in Figure 4, is explained by the increase of dissolved camphor, implying a reduction of the surface tension in the regions between the particles. In fact, measurements of the surface tension in the interparticle regions yielded 69 ± 1.5 mN/m in the case of Figure 4a (phase I) and 66 ± 1 mN/m in the case of Figure 4c (phase III). (The errors are due to the fluctuations in time and space owing to the dynamics of the system.)

An analysis of the translation velocities of whole, single clusters, i.e., considering all the pixel displacements within one cluster, yields Laplacian distributions (Figure 5a) provided that (within the time *T*) the cluster neither attaches to another cluster, nor detaches a part of it, nor changes its shape. If these conditions are not met, we obtain either irregular distributions (Figure 5b) or (in some cases) distributions very close to Maxwellian (Figure 5c).

3.3. Distribution of Minimum Distances. An interesting question is whether the repulsion between the clusters favors a minimum distance between them. This is certainly true for the case of floating, repelling magnets, as investigated in ref 34.

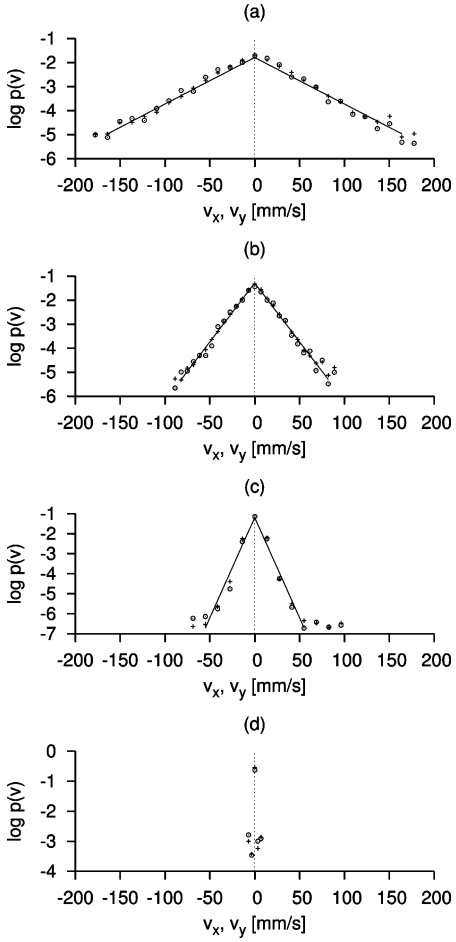

Figure 4. Probability distributions of single pixel velocities v_x (crosses), v_y (circles). Straight lines: fits corresponding to eq 1. (a), (b), (c), and (d) correspond to phases I, II, III, and IV in Figure 2.

To a lesser extent, it is observed for the pigmentation of animal skins (such as cheetahs or zebras in their embryonic stage), where lateral inhibition is caused by chemical morphogens.[35]

In an ideal 2D gas of pointlike particles the probability distribution of the minimal free distance d between a particle and its nearest neighbor is

$$p(d) = 2\pi\eta d\mathrm{e}^{-\pi\eta d^2} \qquad (2)$$

where η is the number of particles per unit area.[36,37] Although eq 2 can be straightforwardly derived, there exists no exact expression for particles of finite size.[37] We restricted ourselves to eq 2 and compared it with experiments for two different ρ-values of phase I (Figure 6). Note that there are no free parameters in eq 2, so that no fit can be performed. In spite of that, we did obtain agreement for large values of d, as shown in Figure 6. In contrast to calculations, however, the experimental values in Figure 6 reveal an interval in the neighborhood of $d = 0$ in which $d \approx 0$. The length of this interval is the effective size d_{eff} of the particles. As an example, for $\rho = 4$ g/m^2, $d_{\mathrm{eff}} \approx 1$ mm (see Figure 6a), which is given by the mean physical diameter $\varphi \approx 0.5$ mm plus a length of repulsion of nearly the same size as φ.

4. Discussion

The ensembles investigated in this work have the unusual feature that they consist of elements with long-range repulsion and short-range attraction. This is also found, for example, in the interactions of nucleons. As a result of the competition of repelling and attracting forces, one obtains different spatial configurations, depending on the density. These configurations range from a gas-like phase to a solid-like phase (phases I through IV). In particular, phase I does merit the denomination "gas-like" because its minimum distance distribution function is comparable to that of an 2D ideal gas (Figure 6).

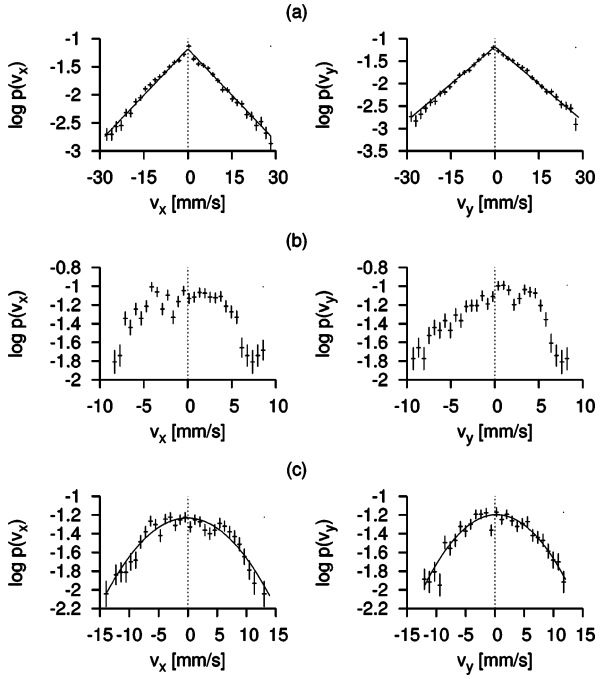

Figure 5. Examples of probability distributions of the velocity components v_x and v_y for different single particles ($\rho = 21$ g/m^2): (a) Laplacian distribution; (b) irregular distribution; and (c) Maxwellian distribution.

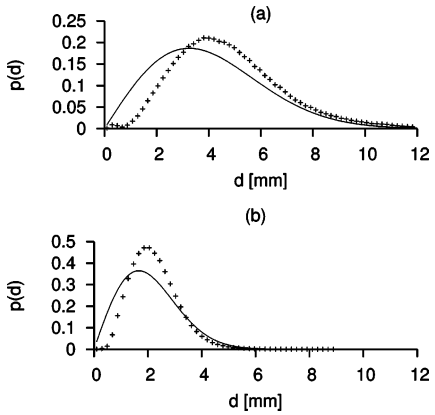

Figure 6. Probability distribution of minimum particle distances: (a) $\rho = 4$ g/m^2 and (b) $\rho = 8$ g/m^2. Continuous curves: Calculations with eq 2. Crosses: Experimental results.

The analysis of the velocity distributions of single pixel displacements yields, surprisingly, Laplacian distributions for all phases I through IV (Figure 4). In contrast, velocities of single clusters may have not only Laplacian, but also other distributions (Figure 5). However, the non-Laplacian behavior of single clusters has no significant effect on the overall distributions shown in Figure 4. It remains an open question whether the occasional Maxwellian distributions of single clusters can be put into a well-defined causal frame. Laplacian distributions have so far been reported in economy (distributions of firm growth rates[38]), ecology (gillnet selection of fishes[39]), grain-size distributions of wheat[40] and sediments,[41] as well as collision-induced absorption spectra.[42] (An overview is found in the book by Kotz et al.[33]) The mechanisms of the systems

found in the literature show no manifest correlations to those of our system. At the present stage of investigations, an explanation of the Laplace distributions we obtained must be left as the subject of future work. Also open are investigations of distributions of positions and velocities at different pH values, ionic strengths, viscosities, and surface concentrations, as has been done for the dynamics of single camphor particles.[13−25]

Acknowledgment. We thank Malte Schmick for valuable help and discussions.

References and Notes

(1) Kline, T. R.; Paxton, W. F.; Wang, Y.; Velegol, D.; Mallouk, T. E.; Sen, A. *J. Am. Chem. Soc.* **2005**, *127*, 11574.

(2) Mano, N.; Heller, A. *J. Am. Chem. Soc.* **2005**, *127*, 11574.

(3) Fournier-Bidoz, S.; Arsenault, A. C.; Manners, I.; Ozin, G. A. *Chem. Commun.* **2005**, 441.

(4) Vicario, J.; Eekelma, R; Browne, W. R.; Meetsma, A.; La Crois, R. M.; Feringa, B. L. *Chem. Commun.* **2005**, 3936.

(5) Paxton, W. F.; Kistler, K. C.; Olmeda, C. C.; Sen, A.; St. Angelo, S. K.; Cao, Y.; Mallouk, T. E.; Lammert, P. E.; Crespi, V. H. *J. Am. Chem. Soc.* **2004**, *126*, 13424.

(6) Chang, S. T.; Paunov, V. N.; Petsev, D. N.; Velev, O. D. *Nat. Mater.* **2007**, *6*, 235.

(7) Magome, N.; Yoshikawa *K. J. Phys. Chem.* **1996**, *100*, 19102.

(8) de Gennes, P. G. *Phys. A* **1998**, *249*, 196.

(9) Nagai, K.; Sumino, Y.; Kitahata, H.; Yoshikawa, K. *Phys. Rev. E* **2005**, *71*, 065301.

(10) Kitahata, H.; Aihara, R.; Magome, N.; Yoshikawa, K. *J. Chem. Phys* **2002**, *116*, 5666.

(11) Ismagilov, R. F.; Schwartz, A.; Bowden, N.; Whitesides, G. M. *Angew. Chem., Int. Ed.* **2002**, *41*, 652.

(12) Nakata, S.; Hiromatsu, S.-I.; Kitahata H. *J. Phys. Chem. B* **2003**, *107*, 10557.

(13) Nakata, S.; Hayashima, Y. *J. Chem. Soc.*,*Faraday Trans.* **1998**, *94*, 3655.

(14) Nakata, S.; Iguchi, Y.; Ose, S.; Ishii, T. *J. Phys. Chem. B* **1998**, *102*, 7425.

(15) Nakata, S.; Hayashima, Y.; Komoto, H. *Phys. Chem. Chem. Phys.* **2000**, *2*, 2395.

(16) Hayashima, Y.; Nagayama, M.; Nakata, S. *J. Phys. Chem. B* **2001**, *105*, 5353.

(17) Nakata, S.; Doi, Y.; Hyashima, Y. *J. Phys. Chem. B* **2002**, *106*, 11681.

(18) Nakata, S.; Doi, Y. *Adv. Compl. Syst.* **2003**, *6*, 127.

(19) Nakata, S.; Doi, Y.; Kitahata, H. J. *Colloid Interface Sci.* **2004**, *279*, 503.

(20) Nagayama, M.; Nakata, S.; Doi, Y.; Hayashima, Y. *Phys. D* **2004**, *194*, 151.

(21) Nakata, S.; Kirisaka, J.; Arima, Y.; Ishii, T. *J. Phys. Chem. B* **2006**, *110*, 21131.

(22) Nakata, S.; Kirisaka, J. *J. Phys. Chem. B* **2006**, *110*, 1856.

(23) Nakata, S.; Kohira, M. I.; Hayashima, Y. *Chem. Phys. Lett.* **2000**, *322*, 419.

(24) Kohira, M. I.; Hayashima, Y.; Nagayama, M.; Nakata, S. *Langmuir* **2001**, *17*, 7124.

(25) Nakata, S.; Doi, Y.; Kitahata, H. *J. Phys. Chem. B* **2005**, *109*, 1798.

(26) Grzybowski, B. A.; Bowden, N.; Arias, F.; Yang, H.; Whitesides, G. M. *J. Phys. Chem. B* **2001**, *105*, 404.

(27) Bowden, N.; Terfort, A.; Carbeck, J.; Whitesides, G. M. *Science* **1997**, *276*, 233.

(28) Terfort, A.; Bowden, N.; Whitesides, G. M. *Nature* **1997**, *386*, 162.

(29) Bowden, N.; Choi, I. S.; Grzybowski, B. A.; Whitesides, G. M. *J. Am. Chem. Soc.* **1999**, *121*, 5373.

(30) Adamson, A. W. *Physical Chemistry of Surfaces*; Interscience: New York, 1976.

(31) Zack, G. W.; Rogers, W. E.; Latt, S. A. *J. Histochem. Cytochem.* **1977**, *25*, 741.

(32) Conklin, G.; Hemami, S. In *In Proceedings of the IEEE Conference on Acoustics, Speech and Signal Processing*; IEEE Computer Soc.: Washington, DC, 1997; Vol. 4.

(33) Kotz, S.; Kozubowski, T. J.; Podgorski, K. *The Laplace distribution and Generalizations*: *a Revisit with Applications to Communications, Economics, Engineering and Finance*; Birkhäuser: Boston, MA, 2001.

(34) Grzybowski, B. A.; Stone, H. A.; Whitesides, G. M. *Nature* **2000**, *405*, 1033.

(35) Murray, J. D. *Mathematical Biology*; Springer: Berlin, Germany, 1989.

(36) Hertz, P. *Math. Ann.* **1909**, *67*, 387.

(37) Torquato, S.; Lu, B.; Rubinstein, J. *J. Phys. A*: *Math. Gen.* **1990**, *23*, L103.

(38) Bottazzi, G.; Secchi, A. *Phys. A* **2003**, *324*, 213.

(39) Porch, C. E.; Fisher, M. R.; McEachron, L. W.; Canad. *J. Fish. Aquatic Sci.* **2002**, *59*, 657.

(40) Sharma, D. L.; D'Antuono, M. F.; Anderson, W. K. *Aust. J. Agric. Res.* **2006**, *57*, 771.

(41) Purkait, B. *J. Sediment. Res.* **2002**, *72*, 367.

(42) Gross, A.; Levine, R. D. *J. Chem. Phys.* **2003**, *119*, 4283.